HHS Public Access

Author manuscript

Acta Biomater. Author manuscript; available in PMC 2018 February 01.

Published in final edited form as:

Acta Biomater. 2017 February ; 49: 272–283. doi:10.1016/j.actbio.2016.11.060.

The Impact of Cell Surface PEGylation and Short-Course Immunotherapy on Islet Graft Survival in an Allogeneic Murine Model

Jaime A. Giraldo[1,2,†], **R. Damaris Molano**[1,3], **Hernán R. Rengifo**[1], **Carmen Fotino**[1], **Kerim M. Gattás-Asfura**[1,4], **Antonello Pileggi**[1,2,3,4,¥], and **Cherie L. Stabler**[1,2,3,4,5,*]

[1]Diabetes Research Institute, University of Miami, Miami, FL, USA

[2]Department of Biomedical Engineering, University of Miami, Miami, FL, USA

[3]Department of Surgery, University of Miami, Miami, FL, USA

[4]Department of Microbiology & Immunology, University of Miami, Miami, FL, USA

[4]Department of Biomedical Engineering, University of Florida, Gainesville, FL USA

Abstract

Islet transplantation is a promising therapy for Type 1 diabetes mellitus; however, host inflammatory and immune responses lead to islet dysfunction and destruction, despite potent systemic immunosuppression. Grafting of poly(ethylene glycol) (PEG) to the periphery of cells or tissues can mitigate inflammation and immune recognition via generation of a steric barrier. Herein, we sought to evaluate the complementary impact of islet PEGylation with a short-course immunotherapy on the survival of fully-MHC mismatched islet allografts (DBA/2 islets into diabetic C57BL/6J recipients). Anti-Lymphocyte Function-associated Antigen 1 (LFA-1) antibody was selected as a complementary, transient, systemic immune monotherapy. Islets were PEGylated via an optimized protocol, with resulting islets exhibiting robust cell viability and function. Following transplantation, a significant subset of diabetic animals receiving PEGylated islets (60%) or anti-LFA-1 antibody (50%) exhibited long-term (> 100 d) normoglycemia. The combinatorial approach proved synergistic, with 78% of the grafts exhibiting euglycemia longterm. Additional studies examining graft cellular infiltrates at early time points characterized the local impact of the transplant protocol on graft survival. Results illustrate the capacity of a simple polymer grafting approach to impart significant immunoprotective effects via modulation of the local transplant environment, while short-term immunotherapy serves to complement this effect.

[*]**Corresponding Author**. Address correspondence to cstabler@bme.ufl.edu.

[†]J.A.G. is currently affiliated with JDRF, New York, NY

[¥]A.P. is currently affiliated with the Center for Scientific Review, National Institutes of Health, Bethesda, MD

Graphical Abstract

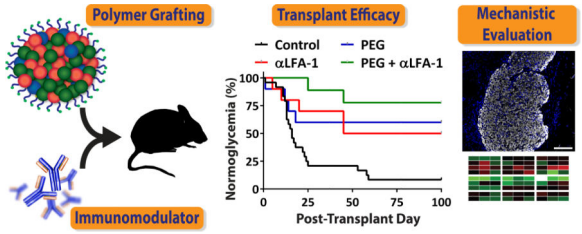

Keywords

polymer grafting; encapsulation; local immunomodulation; poly(ethylene glycol) (PEG); anti-lymphocyte function-associated antigen 1 (LFA-1); inflammation

Introduction

Type 1 diabetes mellitus (T1DM) is an autoimmune disorder characterized by destruction of the insulin producing beta cells within a patient's pancreatic islets of Langerhans [1]. Replacement of beta cells via intraportal infusion of allogeneic islets has the promise of providing a long-term cure for T1DM [2, 3]. Recent clinical islet transplantation (CIT) trials reported sustained improvement in metabolic control, with 57% of patients achieving insulin independence and ~70% with measureable c-peptide levels after 5yrs [3–6]. It has become evident, however, that significant inflammatory and immunological host responses to the islets lead to islet dysfunction and destruction. It has been estimated that as much as 60% of the transplanted islets are lost during the first week due to a potent instant blood-mediated inflammatory reaction (IBMIR), activated when islets are in direct contact with blood [7–9]. Further, despite the use of immunosuppression regimens, a smoldering allogeneic and autoimmune response to the transplanted islets persists, ultimately resulting in rejection [10–13]. Consequently, the development of effective strategies for alleviating early inflammatory events and minimizing the burden of systemic immunosuppression would significantly improve long term efficacy of islet grafts and broaden clinical translation.

Islet encapsulation within biomaterials is an appealing approach to mitigate immunological responses to foreign grafts. Encapsulation consists of creating a biocompatible semipermeable barrier that serves to separate the tissue graft from the host's immune effectors, both cellular and humoral, while permitting the proper diffusion of nutrients such as oxygen and glucose, as well as metabolic waste and therapeutic cell products, such as insulin [14]. Traditional approaches of cell microencapsulation result in a significant void space between the islet and its surrounding environment, leading to hypoxia-induced necrosis and lags in glucose responsiveness, as well as substantial increases in graft volumes that limit implantation site options [15, 16]. Thinner coatings (< 100 micrometers) would minimize these problems, as described in recent publications [17–21], although further optimization and *in vivo* validations are needed.

An alternative approach to full barrier polymeric encapsulation is cell surface modification via poly(ethylene glycol) (PEG) conjugation. PEGylation, the conjugation of PEG to

proteins or cell surfaces, is typically achieved using the heterofunctional PEG: NHS-PEG-CH_3 (NHS-mPEG). The N-hydroxysuccinimide (NHS) group permits spontaneous reactivity to free amines, while the methyl group (CH_3) provides an inert terminal end. It has long been established that the PEGylation of exogenous proteins increases their half-life and reduces immunogenicity without affecting function [22, 23], while PEGylation of cell surfaces, specifically red blood cells, reduces antigenicity *in vitro* and *in vivo* [24]. Overall, PEGylation of the islet cell cluster is a highly attractive approach to mask graft recognition, as this simple and efficient conjugation strategy can easily be performed prior to transplant without altering the transplant procedure (i.e. islets can still be infused into the liver). Given this appeal, islet surface PEGylation has been explored using varying approaches, with minimal adverse effects on islet function or viability observed [25–27]. *In vivo*, however, PEGylation alone has not been shown to significantly extend allograft survival in rodent models, with the exception of a single study exhibiting modest protection using a triple PEGylation procedure [28]. Further, the local impact of PEGylation on host cell responses to allografts has not been studied.

While islet PEGylation as a singular approach has not shown substantial promise, selected studies have demonstrated a synergistic impact when combined with low-dose or local immunosuppression [29–31]. In this study, we sought to explore the impact of a targeted and short-course immune intervention used in combination with islet PEGylation. Lymphocyte Function-associated Antigen-1 (LFA-1) is a surface integrin found on immune cells involved in cell trafficking to sites of injury and/or infection, immune synapse stabilization, and co-stimulation [32]. LFA-1 blockade as a monotherapy has demonstrated success in delaying, but not completely preventing, murine allograft rejection [33]. Further, it has shown to be synergistic with other immune interventions [34–37]. Herein, the effects of PEGylation, alone or in combination with a short-course LFA-1 blockade, on graft survival and the local impact on host cell phenotypes were explored.

Materials and Methods

Reagents and Polymer Fabrication

All chemical reagents were purchased from Sigma-Aldrich, unless otherwise noted. All culture media was sourced from Mediatech.

Fabrication of NHS-PEG-CH_3

NHS-PEG-CH_3 was fabricated by dissolving NH_2-PEG-CH_3 (2 g, JenKem Technology USA, MW 5000 Da) in 4 mL of anhydrous N,N'-dimethylformamide (DMF) at 37 °C under Argon. A solution consisting of glutaric anhydride (50 mg) dissolved in 0.4 mL DMF was then injected drop-wise into the PEG solution, followed by drop-wise injection of a solution consisting of 112 μL triethylamine in 0.4 mL DMF. After stirring for 25 min, the product (COOH-PEG-CH_3) was precipitated with 60 mL cold diethyl ether, collected by centrifugation, and dissolved in 60 mL absolute ethanol at 37 °C. The solution was then filtered through a 5 mm silica gel plug inside a Pasteur pipet and the polymer was precipitated and collected by cooling in an ice-water bath and centrifugation. This product

was rinsed by vortex-shaking with 60 mL cold diethyl ether, collected by centrifugation, and dried under reduced pressure.

The above product (925 mg) and N-hydroxysuccinimide (65 mg) were dissolved in 1.5 mL DMF at 37 °C under Argon. A solution of 176 μL diisopropylcarbodiimide (AnaSpec) was dissolved in 0.4 mL DMF and injected to the PEG solution. After stirring for 2 h under Argon, the product was precipitated with 40 mL cold diethyl ether and collected by centrifugation. This was subsequently dissolved in 32 mL absolute ethanol at 37 °C, precipitated by cooling in an ice-water bath, and collected by centrifugation. The product was rinsed with 40 mL cold diethyl ether, collected by centrifugation, and dried under reduced pressure. The final yield was 900 mg of NHS-mPEG powder. Chemical modifications throughout this process were monitored by FT-IR.

Islet Isolation and Culture

Studies involving animals were performed under protocols reviewed and approved by the University of Miami IACUC. Male DBA/2J (H-2^d) mice, between 10–12 weeks of age (Jackson Laboratory; Bar Harbor, Maine), were used as islet donors. Islets were isolated as previously described, counted, and scored for size using the islet equivalent (IEQ) method [38]. Islets were cultured at 37 °C, 5% CO_2 in CMRL 1066-based medium supplemented with 10% FBS, 20 mM Hepes Buffer, 1% penicillin-streptomycin, and 1% L-glutamine.

PEGylation

Isolated islets were cultured for 48 h prior to PEGylation. On the day of the procedure, islets were counted, washed thrice in DPBS, and incubated for 45 minutes at 37 °C in a freshly prepared 4 mM NHS-mPEG solution in DPBS (titrated to pH 7.8 before addition of mPEG) supplemented with Ca^{2+}/Mg^{2+} and 11 mM D-glucose at a cell density of 1500 IEQ/mL. Following PEGylation, the islets were washed thrice in full media and placed in the incubator for overnight culture prior to assessment or transplantation. For imaging of islet coating, NHS-PEG-FITC (5,000 MW, NANOCS Co) was used in lieu of NHS-mPEG.

In-vitro Islet Characterization

The grafting of PEG to the islet surface was confirmed through the visualization of NHS-PEG-FITC. Islets were imaged 24 h after conjugation on a Leica SP5 inverted confocal microscope. Single plane images and merged multi-slice images (4–8 μm thickness; 8–15 slices per image; 1024×1024; 20× objective) were collected. Islets were counterstained with Hoescht 33342 dye for cell nucleus visualization.

Islet viability and function were evaluated 24 hr post-PEGylation using Live/Dead imaging and glucose stimulated insulin secretion. Cell viability was visualized via LIVE/DEAD Viability/Cytotoxicity Assay Kit (Invitrogen) and imaged through a Leica SP5 Inverted Confocal Microscope. Islets were briefly rinsed in HBSS once and incubated for 60–90 min in a DPBS composed of 4 μM calcein AM and 8 μM ethidium homodimer-1 (EthD-1) as previously described [39]. Islets were then rinsed in DPBS, placed on cover slips, and multi-slice images (4–8 μm thickness) were collected and compiled using the maximum intensity projection function in ImageJ. A dynamic glucose stimulated insulin release (GSIR) study

was conducted using a perifusion machine (Biorep), as previously described [40]. Islets (50 handpicked) were stimulated according to the following series: 10 min low glucose (3 mM), 20 min high glucose (11 mM), 10 min low glucose, 5 min KCL (25 mM), and 10 min low glucose. Insulin concentration was measured using an insulin ELISA (Mercodia).

Islet Transplantation and Graft Assessment

Male C57BL/6J (H-2^b) mice, between 7–9 weeks of age (Jackson Laboratory), were used as transplant recipients. Mice were rendered diabetic by IV streptozotocin injection, as previously described [21] and were used as transplant recipients after 3 consecutive readings confirming non-fasting blood glucose levels > 350 mg/dL. Islets (700 – 800 IEQ/recipient) were transplanted in the kidney subcapsular space of anesthetized mice, as previously described [34, 41, 42]. This dosage, which was higher than a standard IEQ, was used to increase the likelihood of prompt reversal to euglycemia within 48 h post-transplant, as efficient reversal ensured adequate delineation from primary nonfunction and islet rejection. Four groups were tested: (1) animals receiving untreated islets with saline (saline control group; n = 27); (2) animals receiving untreated islets and short-course anti-LFA-1 antibody (KBA clone, 100 μg/day, i.p. on days 0 – 6; LFA-1 blockade group; n = 10) [43]; (3) animals receiving PEGylated islets and saline (PEGylated islet group; n = 11); and (4) animals receiving PEGylated islets in conjunction with short-course αLFA-1 antibody (combination LFA-1 blockade and PEGylated islets group; n = 13). Normoglycemia was defined as non-fasting glycemic levels < 200 mg/dL for 2 consecutive days. Mice that remained hyperglycemic for over 10 d following transplant were classified as Primary Non-function (PNF), euthanized, and excluded from further analysis. Graft rejection was defined as functional grafts that exhibited diabetes recurrence, defined as the day glycemic levels > 300 mg/dL were detected. After at least 3 days of confirmed hyperglycemia, the animal was euthanized and the graft explanted for analysis. All graft-bearing kidneys from animals displaying sustained normoglycemia long-term (> 100 d) were electively explanted in a survival nephrectomy to confirm subsequent diabetes status of recipients. Explanted kidneys were fixed in 10% formalin solution, embedded in paraffin, and cut into 5 μm sections for histopathological analyses.

For immunofluorescence microscopy analyses, slides from long-term functioning grafts were treated via antigen retrieval following de-paraffinization using EDTA Decloaker 5× (Biocare Medical), and blocking was carried out for 2 and 1 h with Power Block Universal Blocking Reagent (BioGenex) and Protein Block (BioGenex), respectively. Primary antibodies, anti-CD3 (Cell Marque; 1:50) and anti-FoxP3 (eBiosciences; 1:100), were incubated overnight at 4 °C, followed by rinsing and addition of appropriate fluorochrome-labeled secondary antibodies. Next, sections were washed and incubated with Insulin (Dako; 1:100) primary antibody, followed by washes and appropriate secondary antibody incubation. Nuclear counterstaining was perfomed with DAPI and samples were subsequently sealed.

Short Term Studies

For examination of the local implant site, additional transplants with the same treatment groups were performed and mice were euthanized on 4, 8, and 15 d post-transplantation (n =

4 for each time point and each group, total of 48 samples). At the designated time point, the explanted graft bearing kidney was flash frozen in OCT and sections (10 μm; 2/slide) were mounted onto both glass (for immunohistochemistry) and RNAse-free PEN membrane slides (for laser-capture microdissection (LCM). In order to capture samples that represent the entire graft, sections were collected in 5 cycles with 4 glass slides (for IHC) and 2 membrane slides (for LCM) for a total depth of 120 μm sampled for each cycle (600 μm total); permitting sample collection from different regions of the graft for analysis. This resulted in 20 glass slides for IHC and 10 membrane slides for LCM per animal per group per time point. Extensive cleaning of stage and new blades (100% EtOH and RNAse Away) was done between each kidney to prevent cross-sample contamination. Sections were kept on dry ice during the collection procedure and stored at −80 °C until processed.

Slides designated for immunohistochemistry were subjected to hematoxylin and eosin (H&E), Masson's Tri-Chrome, or immunofluorescence staining. For immunofluorescence staining, slides were fixed in paraformaldehyde (PFA) solution for 5 minutes, rehydrated, and blocked as described above. Primary and secondary antibodies were incubated at 4 °C overnight and at room temperature for 1 h, respectively. Primary antibodies and dilutions used include anti-CD68 (AbD Serotec; 1:200) as a general macrophage marker, anti-CD206 (Santa Cruz Biotech; 1:100) as an M2 macrophage marker, and anti-Insulin (Dako; 1:100) for beta cells [44]. Nuclei were counterstained using DAPI (Invitrogen; 1:5000) and samples were subsequently sealed. For all immunofluorescence studies, all stains were compared to isotype controls (primary antibody omitted) to ensure specificity of detection. Entire slide sections were imaged using a Leica SP5 Inverted Confocal Microscope and quantification of targeted cells (CD68 and CD206 cells) was made using ImageJ (NIH) from defined ROI ($n > 15$) within the transplanted sections.

For slides designated for qPCR, the graft was identified and LCM was performed using the Histogene® LCM Frozen Section Staining Kit (Applied Biosystems) following manufacturer's instructions. Stained PEN membrane slides were kept in a vacuum chamber filled with drierite to absorb ambient moisture in order to prevent degradation of the retrieved RNA and LCM was carried out immediately after staining using a Leica AS LMD microscope. The LCM station was thoroughly cleaned with 100% ethanol and RNAse Away before each dissection. The identified graft was cut from each section, with all microdissected samples from a given graft/animal being collected into a single tube. Thus, samples were pooled to provide an RNA signature from each recipient animal tested, resulting in $n = 4$ samples per group per time point. RNA extraction buffer (PicoPure RNA Isolation Kit, Applied Biosystems) was added, incubated at 42 °C for 30 min, and stored at −80 °C. Subsequently, RNA was isolated per manufacturer's instructions, treated using Turbo DNA-free Kit (Invitrogen), and stored at −80 °C.

RNA isolated from LCM sections were preamplified using the Arcturus™ RiboAmp® PLUS Kit (Applied Biosystems) following the manufacturer's instructions, followed by treatment with the Turbo DNA-free. cDNA was synthesized using the High Capacity cDNA Reverse Transcription Kit with RNase Inhibitor (Applied Biosystems; 25 ng/ul of RNA), following the manufacturer's instructions. qPCR reactions were carried out using TaqMan reagents and the 2× TaqMan Fast Universal PCR Master Mix (Applied Biosystems; 3 μL

cDNA). Elimination of genomic DNA contamination or cDNA remnants from the preamplification procedure was confirmed by performing PCR reactions with cDNA samples generated without the Reverse Transcriptase (No-RT samples) and the 18s primer prior to full sample analysis. qPCR analysis was then performed for the primers listed in Table 1. Reactions were carried out for 40 cycles in a StepOnePlus Real-Time PCR System (Applied Biosystems), outlier replicates were removed using the ExpressionSuite Software (Applied Biosystems/Life Technologies), and relative gene expression analysis was done using the $2^{(-dCt)}$ comparative method and expressed as fold change, as previously published [45], comparing experimental groups to the control group from the corresponding time point. In cases were the target genes in control samples were undetected, a Ct of 40 was substituted to permit comparative analysis.

Statistical Analysis

For *in vitro* studies, comparisons between groups were made using the same islet preparation, with a minimum of three independent replicate measurements for each assay. Results are expressed as the mean ± SD. A minimum of three independent experiments (e.g. three islet isolations) were performed for each assessment, with graphs summarizing results from a representative experiment (with triplicates run for each measurement). Statistical analyses for islet viability and insulin secretion experiments used multi-factor analysis of variance, with student t-tests for comparison between individual groups. For *in vivo* studies, efficacy transplants were conducted via 4 independent isolations and transplant experiments, with all groups included, in varying numbers, for each experiment, while short-term studies were conducted in 4 separate isolations/transplant experiments. For time to reversal analysis (% normoglycemia), Mantel-Cox (logrank) test was performed to evaluate differences between groups. qPCR data was analyzed by determination of the amount of target gene expression relative to the B-Actin endogenous gene control for each sample and performing a Kruskal-Wallis non-parametric one way ANOVA followed by a Dunn's post-test to compare the different treatment groups. For all studies, differences were considered significant when $P < 0.05$.

Results

In vitro assessments of islet function following PEGylation

In this study, PEGylation of the islet cluster was achieved via grafting high molecular weight NHS-PEG-CH_3, whereby the N-hydroxysuccinimide (NHS) group on the PEG chain spontaneously reacts with primary amines to yield a stable amide bond. A high MW PEG was used to promote binding to the periphery of the islets, particularly to the extracellular matrix (ECM) that develops on the outside of the islet, which is rich in free amines. In an effort to maximize PEG grafting to this matrix, islets were PEGylated 48 h after enzymatic isolation to permit regeneration of the ECM [46]. The incubation conditions during the 45 min PEG grafting procedure, such as pH and temperature, were tailored to optimize the NHS reaction while mitigating impacts on islet viability and function. To visually assess the grafting of PEG to the surface of the islet, a fluorescein labeled PEG (NHS-PEG-FITC) was used. Confocal microscope images revealed a high degree of polymer grafting with positive fluorescence across the entire islet surface; establishing complete PEG grafting to the whole

cellular spheroid. Areas of high intensity fluorescence were also seen, however, indicating clustering of PEG chains in selected sections (Figure 1A–C). Further, PEG conjugation was relegated to the periphery of the islet, as highlighted by images collected near the center of the 3-D islet (Figure 1D). Of note, the gradient of fluorescence observed from the periphery of the islet towards the center is a result of laser absorption and scattering from the dense 3-D islet cluster. The variable clustering of PEG chains at the margins of the pancreatic islet cluster suggest PEG binding to the amine-rich ECM. This would account for the observed variability in clustering patterns, as deviations in the stripping of the native ECM during the enzymatic digestion of the pancreas, as well as disparities in the rebuilding of this matrix during culture, results in unpredictable peri-islet ECM deposition [46].

Following PEGylation, the viability and function of the coated islets were assessed by live/dead imaging and glucose simulated insulin release, respectively. As shown in Figure 1 (E–F), highly viable islets were observed following PEGylation, with no discernible elevation in dead cells. Islet function following PEGylation was evaluated via dynamic glucose stimulated insulin release. Dynamic glucose stimulation was conducted to capture the impact of PEG grafting on the responsiveness of the islets to a glucose challenge. In this manner, control (untreated) and PEGylated islets were exposed to step changes in glucose (i.e. low (3 mM), high (11 mM), and then low (3 mM)) and the perifused media was collected every minute to capture the dynamics of insulin release. To characterize the amount of insulin within the islet following stimulation, the islets were then treated with KCL, which results in a burst release of insulin due to membrane depolarization. For control islets, a healthy stimulation curve was observed, with prompt, biphasic stimulation during the high glucose challenge (AUC = 58.9 ± 21.3) and robust insulin release following KCL-induced membrane depolarization (peak insulin 6.5 ± 1.9 μg/L) (Figure 1G). For PEGylated islets, the insulin release pattern of biphasic stimulation (AUC = 69.07 ± 4.62) and insulin release during KCL stimulation (7.04 ± 1.1 μg/L) was statistically identical to control islets ($P = 0.46$ and 0.69, respectively); demonstrating no delay or dampening in their response to a dynamic glucose challenge. Taken together, the data demonstrate that the grafting of PEG chains to the islet surface, using these optimized conditions, results in no detrimental impacts on islet viability or function.

Immunoprotection of PEGylated islets and Complementary Impact of Short-Course Immunotherapy in a Full MHC Mismatched Murine Model

To investigate the potential of islet PEGylation to confer immunoprotection and improve allograft outcomes, DBA/2J (H-2^d) islets were implanted into fully MHC mismatched C57BL/6J (H-2^b) recipients. Following transplantation, 24 of the 27 (89%) mice receiving control islets and 10 of the 11 (91%) mice receiving PEGylated islets achieved normoglycemia. No statistical difference in function between control and PEGylated islets was observed ($P = 0.85$). As shown in Figure 2A, 92% of the functional control islet transplants rejected within 30 d, with 2 transplants exhibiting normoglycemia over 100 days post-transplant. For recipients of PEGylated islets, a significant increase in the number of grafts exhibiting long-term function was observed when compared to controls, with 6 of the 10 grafts (60%) demonstrating stable euglycemia for over 100 days post-transplant ($P < 0.01$). The 4 rejected PEGylated islet grafts destabilized within the first 20 d.

To evaluate if combining short-course immunotherapy with islet PEGylation would improve immunoprotection, anti-LFA-1 antibody (100 μg/d) was given as a short-course immunosuppressant on days 0–6 [34]. Groups received anti-LFA-1 monotherapy and either unmodified or PEGylated islets. Following transplantation, all 10 of the 10 (100%) recipients of unmodified islets with anti-LFA-1 and 9 of the 13 (69%) mice receiving PEGylated islets with anti-LFA-1 reverted to normoglycemia. There was no statistical elevation in PNF for the combination group (PEGylated islets plus anti-LFA-1) when compared to controls ($P = 0.13$). As shown in Figure 2B, 50% of the recipients of unmodified islets and anti-LFA-1 displayed stable allograft function for over 100 d ($P = 0.022$, compared to control), which is equivalent to the level of protection observed for PEGylated islet transplants ($P = 0.80$). When PEGylated islets were paired with systemic anti-LFA-1, graft survival was significantly increased to 78% ($P = 0.0003$, compared to control). The two rejected grafts from this combinatory group destabilized at later time points (25 and 45 d post-transplant). The time of rejection for functional grafts averaged 11 days for the PEGylated islet group, 25 days for those receiving anti-LFA-1, and 35 days for the combination treatment group. As such, PEGylated grafts trended towards rejection at early stages, while the addition of anti-LFA-1 delayed rejection.

Survival nephrectomies of the long-term functional grafts resulted in hyperglycemia, validating the efficacy of the transplanted islets. Representative tri-chrome and insulin stained sections of explanted grafts correlated with graft function. While control islets (20 d post-transplant) clearly exhibited destruction of the islet graft by immune infiltrates and a waning presence in insulin (Figure 2 C, G), grafts from treated groups (PEGylated islets, α-LFA-1, and PEGylated islets + α-LFA-1) showed preserved islet cytoarchitecture and insulin-positive cells, even after > 190 days post-transplant (Figure 2 D–F & H–J).

Immunological Evaluation of Long-Term Grafts

Immunopathological evaluation of T cells was performed on long-term functioning grafts within treated groups. Most grafts showed minimal presence of T cells (Figure 3 A–B) with sporadic $CD3^+$ cells related to the periphery of the islet. For selected grafts treated with the combination of anti-LFA-1 and PEGylated islets, a higher number of $CD3^+FoxP3^+$ cells, classically identified as T regulatory cells (T_{regs}), was observed (Figure 3 C–D). Additionally, for selected functional grafts in all treated groups, pockets of mononuclear cell accumulation, with a strong proportion of $CD3^+FoxP3^+$ cells, were observed (Figure 3 E–F). The infiltrate appeared confined at the periphery of the allograft, where islets adjacent to the mononuclear cells remained intact with no notable intra-islet infiltration or loss of insulin expression.

Short-Term Effects of PEGylation and LFA-1 Blockade on the Immune Response

To explore how PEGylation and/or LFA-1 blockade may modulate early host responses to encourage long-term graft acceptance, additional transplants were conducted with elective explants on 4, 8, and 15 d post-transplantation. These grafts were then characterized via microdissection and subsequent gene analysis on the isolated tissue and immunohistochemical staining.

Genes selected for this study sought to elucidate the nature of the host response as a result of different treatments, with a focus on cellular infiltration and pro- or anti-inflammatory cytokines. For cellular infiltration into the graft area, CD45, CD3, F4/80, and Klrb1C, as markers of general immune cell infiltrate, T-cells, macrophages, and NK cells, respectively, were measured. To gauge the pro-inflammatory nature of the microenvironment, granzyme B (GzmB), interferon gamma (IFNγ), and tumor necrosis factor alpha (TNF-α) were measured. For anti-inflammatory markers, transforming growth factor beta (TGF-β) and interleukin 10 (IL-10) were quantified. Results, expressed as fold change from control, revealed interesting trends in gene expression between groups over time (Figure 4A). Overall, treatment via PEGylation of islets and/or short-course systemic LFA-1 blockade resulted in decreased general immune cell recruitment ($CD45^+$ cells) to the graft and suppression of pro-inflammatory cytokines during the early stage of engraftment (day 4). While the arrest of $CD45^+$ cell recruitment was not sustained past day 4, the dampening of pro-inflammatory cytokines persisted over 2 weeks post-transplant. Of interest, macrophage recruitment was increased for all groups at early time points, particularly the PEGylated islet group. The combinatory group (PEG+anti-LFA-1) exhibited significant upregulation of macrophages only after 15 days post-transplant. Further, suppression of pro-inflammatory factors did not generally translate to upregulation of anti-inflammatory cytokines, although TGF-β was significantly upregulated for most groups across all time points, with the exception of the combination group on day 4.

Due to the interesting trend of macrophage recruitment, immunofluorescent staining for the macrophage marker CD68 and the M2 macrophage marker CD206 was conducted at day 8 (Figure 4B–E). In control samples, $CD68^+$ cells that were primarily $CD206^-$ were observed. Both the anti-LFA-1 group and the PEGylated islet group exhibited a similar trend of $CD68^+CD206^-$ cell presence (Figure 4 C & D, respectively). Examination of the interaction of macrophages with the allogeneic islets, however, revealed some differences. For control groups, macrophages appeared to be actively infiltrating the insulin-positive islets (Figure 4B, right panel), while the anti-LFA-1 and the PEGylated islet groups illustrated macrophages relegated to the islet periphery. For the combination (anti-LFA-1 + PEG) group, the number of $CD68^+$ cells within the graft area was comparable to control transplants, but most of these macrophages appeared to co-express $CD206^+$, hence exhibiting an M2 phenotype. These cells also did not appear to be infiltrating the islet (Figure 4E). Image analysis of these sections (Figure 4F–G) revealed no significant changes in macrophage presence in the graft, except for the anti-LFA-1 group, which was significantly decreased. Characterization of CD206+ macrophages found a significant increase in cells exhibiting this M2 phenotype within the combinatory (PEG +anti-LFA-1) group.

Discussion

The PEGylation of surfaces has long been known to reduce protein adsorption and cell attachment [24, 47]. This property makes PEG a promising candidate to mitigate inflammation during the early transplant period by reducing both the adsorption of plasma proteins onto the islet surface, which instigates cell attachment, and the exposure of inflammatory markers such as tissue factor, which initiates the coagulation cascade. Further,

PEG has been used to immunocamouflage cellular transplants by masking cell surface antigens to prevent T cell recognition and activation [24, 47]. Although grafting of PEG to the islet surface alone did not confer complete protection of the graft from the host's immune response, this simple conjugation strategy provided a barrier that lead to a significant impact on overall rejection rates. Additionally, a potential beneficial effect of the PEG coating on the islet cluster might be in the stabilization of peri-insular ECM moieties, which reduce anoikis of islet cells and danger signals following transplantation [48]. It is worth noting that the extrahepatic implantation site of the renal subcapsular space likely experiences a degree of inflammation substantially lower to that of the intrahepatic site, where IBMIR plays a significant role in declining graft survival. Thus the benefits of PEGylation may be more pronounced when used in this clinically relevant site, particularly given the documented impact of PEG chains on decreasing surface activated inflammation [49, 50].

The comparison of PEG grafting with immunosuppressive monotherapies, both historical (e.g. cyclosporine, rapamycin, CTLA4-Ig, and CD40L mAb [51–53]) and the anti-LFA-1 used in this study, found that this optimized islet PEGyation technique could offer an alternative that provides equivalent protection while minimizing the clinical risks associated with immunosuppressive drugs [3, 43, 54–56]. Further, the combination of PEG with a short-course immunotherapy significantly decreased graft rejection, indicating that the addition of PEGylated islets to current immunosuppressive regimens could result in an improvement in overall transplant outcomes.

Of note, control grafts for this complete MHC mismatch allogeneic murine transplant exhibited long-term acceptance of grafts in 2 of the 24 transplants. While treatment groups demonstrated a significant and substantial increase in graft survival, indicating the robust nature of our conclusions regarding the benefits of the treatments utilized, the incidence of long-term acceptance in 8% of the grafts may call into question the strength of this particular allograft model. As such, it is important to clarify that the rejection of allogenic islets can be dampened with extended culture times and/or preconditioning via induction of cytoprotective molecules, due to loss in passenger leukocytes and MHC Class II expressing cells during *in vitro* culture [57–59]. The extended culture of islets for this study (i.e., 3-fold longer than the standard 24 hours post-isolation) likely contributed to the lack of complete rejection of all control grafts for this mismatched strain.

Examination of early host responses to treatment groups suggest a mechanism in which the migration of immune cells to the graft site is delayed. As supported in previous publications, delayed migration of immune cells was observed with the use of anti-LFA-1 [43, 56]. Further, inflammatory cytokines resulting from activated T, B, or NK cells were suppressed for treatment groups, indicating decreased effector immune cells and subsequent activation of macrophages towards an M2 phenotype. Inhibiting the production of inflammatory cytokines during the early stages of engraftment, as observed for all treatment groups, has been strongly correlated with improved islet engraftment and sustainment of graft duration in clinical allograft islet transplants [60–62].

The role of macrophages in early engraftment was examined by both gene expression analysis and immunohistochemistry, as these cells are critical players in modulating early inflammation, engraftment, and beta cell replication [63], as well as in T cell-mediated and antibody-mediated rejection [64, 65]. For qPCR analysis, all treatment groups demonstrated increased macrophage presence within the graft, while image analysis of explanted grafts indicated minimal differences and even suppression for the anti-LFA-1 group. This disparity may be attributed to the different markers utilized to detect macrophages (F4/80 vs CD68) and the technique of measurement (qPCR vs IHC). Macrophage infiltration into the islets for animals receiving either PEGylated islets or systemic anti-LFA-1 treated grafts, however, was strongly impaired when compared to control grafts, demonstrating that the treatment either impaired infiltration via physical barrier, as in the case of the PEG grafts, or via dampened activation due to anti-LFA-1 destabilization of the immune synapse [66]. Given the critical role of macrophage allograft infiltration in rejection and the published correlation between dampened macrophage infiltration and increased islet allograft acceptance, suppression of this migration likely played a role in supporting long-term acceptance of these fully MHC-mismatched allografts [67–70].

For the combination PEG + α-LFA-1 group, the role of macrophages in the graft microenvironment appeared to be characteristically different. While general macrophage migration was not up-regulated on day 8, as supported by both qPCR and IHC analysis, these macrophages exhibited significant co-expression of CD206 in IHC-analyzed grafts, illustrating a significant shift towards an M2 phenotype. Of note, qPCR primers used to classify macrophage phenotype (i.e. Nos2 for M1 and Sphk1 for M2) for gene analysis were not successful, thus this method could not be used to validate IHC observations. Overall, the increased presence of M2 macrophages in this combination treatment group likely conferred the improved observed benefits, by promoting engraftment while dampening TH1 responses [71].

In addition to modulation of innate immune responses, an elevated presence of $FoxP3^+$ T cells, classified as T regulatory cells (T_{reg}), was observed for long-term grafts treated with the combination of PEGylated islets + α-LFA-1. This observation correlates with the observed increase in M2 macrophages at the graft site, as M2 macrophages are known to induce phenotype switching of T cells from an effector towards a regulatory phenotype [72, 73]. These inducible Tregs, e.g. regulatory T cells induced in the periphery, have been associated with enhanced allograft survival via tolerance pathways [74, 75]. Additionally, the observed clusters of Treg-containing lymphocytic pockets in long-term functioning grafts have been commonly detected in long-term grafts when pharmacological agents (such as anti-LFA-1) and polymeric brushes were employed [21, 51, 52]; further indicating a regulatory component to the successful grafts.

Even with the combination of PEGylation and short-course immunotherapy, there was still a selected cohort (2 grafts) that rejected, albeit at delayed times of 25 and 45 days post-transplant. Why these two grafts rejected, while the others did not, cannot be attributed to any known factors associated with the islet isolation or recipient group. This is not unlike clinical islet transplantation, where no correlation, to date, has been found between a pre-

transplant islet assay(s) or the recipient's profile and the overall transplant outcome or graft duration [76]. Thus, identification of such factors is the focus of numerous research studies.

As islet PEGylation alone was not sufficient to completely protect all islet grafts from rejection, future studies will seek to improve the polymeric surface modification approach, through either improving PEG graft density or adding polymeric layers. PEG graft density could be enriched via additional PEG grafting steps [28], supporting ECM capsule regeneration, or supplementation of free amines on the islet surface. Further, examination of dosage requirements in murine allografts will seek to explore the impact of antigen dosage (via islet mass) on rejection rates. Alternatively, formation of multi-layer coatings via layer-by-layer approaches may result in more predictable and uniform coatings capable of complete islet encapsulation [20, 21, 77–79]. While new approaches are being developed, the simplicity of the PEGylation procedure, the lack of complex polymer fabrication or instrumentation required, the capacity to still utilize the intrahepatic site, and the predicted ease in regulatory approval due to the pervasive use of PEG in pharmaceuticals makes this an attractive approach for mitigating host responses to islet transplants, which can easily be incorporated into current transplantation protocols. As such, on-going studies are exploring the potential of islet PEGylation, in combination with conventional clinical islet immunosuppressive regimens, to improve long-term graft outcomes in larger animal models.

Conclusion

In our study, PEGylation of the islet surface was confirmed and shown to have no adverse effect on islet viability or function. *In vivo* experiments were subsequently pursued to assess the effects of PEGylation on long-term islet graft survival. Transplant studies clearly demonstrated the capacity of islet PEGylation to confer modest protection from immune attack in a full MHC mismatched mouse model, with transplant survival comparable to that observed for short-course LFA-1 blockade monotherapy. Furthermore, it was shown that the combination of PEGylation and LFA-1 blockade resulted in a complementary effect that elevated graft survival rates to 78%. Analysis of the graft microenvironment revealed a role for immune cell suppression on graft function, as well as macrophage infiltration and phenotype. Overall, this simple approach provides a useful and benign tool in the toolbox of immunomodulatory agents for dampening inflammatory and immunological responses to islet allografts.

Acknowledgments

This work was supported by the National Institutes of Health (1DP2 DK08309601 and R01DK100654) and the Diabetes Research Institute Foundation. Dr. Rengifo was supported by an NIH Postdoctoral Supplement (1DP2 DK08309601-02/03). We thank the DRI Preclinical and Translational Models Core for providing the rodent islets used for this study and for the care, maintenance, and transplantation of the islets and animals for *in vivo* assessment. We thank Kevin Johnson in the DRI Histological Core for his histological prowess and training. We thank Nicholas Abuid for collection of PEGylated islet confocal images. We thank the DRI Analytical Imaging and Histology Cores for use of their facilities.

Dr. Giraldo is currently employed at JDRF, New York, NY and Dr. Pileggi is currently employed at the National Institutes of Health (NIH).

References

1. Mathis D, Vence L, Benoist C. Beta-cell death during progression to diabetes. Nature. 2001; 414(6865):792–798. [PubMed: 11742411]
2. Shapiro AM, Lakey JR. Future trends in islet cell transplantation. Diabetes Technol Ther. 2000; 2(3):449–452. [PubMed: 11467347]
3. Shapiro AM, Ricordi C, Hering BJ, Auchincloss H, Lindblad R, Robertson RP, Secchi A, Brendel MD, Berney T, Brennan DC, Cagliero E, Alejandro R, Ryan EA, DiMercurio B, Morel P, Polonsky KS, Reems JA, Bretzel RG, Bertuzzi F, Froud T, Kandaswamy R, Sutherland DE, Eisenbarth G, Segal M, Preiksaitis J, Korbutt GS, Barton FB, Viviano L, Seyfert-Margolis V, Bluestone J, Lakey JR. International trial of the Edmonton protocol for islet transplantation. N Engl J Med. 2006; 355(13):1318–1330. [PubMed: 17005949]
4. Tharavanij T, Betancourt A, Messinger S, Cure P, Leitao CB, Baidal DA, Froud T, Ricordi C, Alejandro R. Improved long-term health-related quality of life after islet transplantation. Transplantation. 2008; 86(9):1161–1167. [PubMed: 19005394]
5. Cure P, Pileggi A, Froud T, Messinger S, Faradji RN, Baidal DA, Cardani R, Curry A, Poggioli R, Pugliese A, Betancourt A, Esquenazi V, Ciancio G, Selvaggi G, Burke GW 3rd, Ricordi C, Alejandro R. Improved metabolic control and quality of life in seven patients with type 1 diabetes following islet after kidney transplantation. Transplantation. 2008; 85(6):801–812. [PubMed: 18360260]
6. Hering BJ, Clarke WR, Bridges ND, Eggerman TL, Alejandro R, Bellin MD, Chaloner K, Czarniecki CW, Goldstein JS, Hunsicker LG, Kaufman DB, Korsgren O, Larsen CP, Luo X, Markmann JF, Naji A, Oberholzer J, Posselt AM, Rickels MR, Ricordi C, Robien MA, Senior PA, Shapiro AM, Stock PG, Turgeon NA. Phase 3 Trial of Transplantation of Human Islets in Type 1 Diabetes Complicated by Severe Hypoglycemia. Diabetes Care. 2016; 39(7):1230–1240. [PubMed: 27208344]
7. Biarnes M, Montolio M, Nacher V, Raurell M, Soler J, Montanya E. Beta-cell death and mass in syngeneically transplanted islets exposed to short- and long-term hyperglycemia. Diabetes. 2002; 51(1):66–72. [PubMed: 11756324]
8. Mattsson G, Jansson L, Nordin A, Andersson A, Carlsson PO. Evidence of functional impairment of syngeneically transplanted mouse pancreatic islets retrieved from the liver. Diabetes. 2004; 53(4): 948–954. [PubMed: 15047609]
9. Ozmen L, Ekdahl KN, Elgue G, Larsson R, Korsgren O, Nilsson B. Inhibition of thrombin abrogates the instant blood-mediated inflammatory reaction triggered by isolated human islets: possible application of the thrombin inhibitor melagatran in clinical islet transplantation. Diabetes. 2002; 51(6):1779–1784. [PubMed: 12031965]
10. Cardani R, Pileggi A, Ricordi C, Gomez C, Baidal DA, Ponte GG, Mineo D, Faradji RN, Froud T, Ciancio G, Esquenazi V, Burke GW 3rd, Selvaggi G, Miller J, Kenyon NS, Alejandro R. Allosensitization of islet allograft recipients. Transplantation. 2007; 84(11):1413–1427. [PubMed: 18091517]
11. Huurman VA, Velthuis JH, Hilbrands R, Tree TI, Gillard P, van der Meer-Prins PM, Duinkerken G, Pinkse GG, Keymeulen B, Roelen DL, Claas FH, Pipeleers DG, Roep BO. Allograft-specific cytokine profiles associate with clinical outcome after islet cell transplantation. Am J Transplant. 2009; 9(2):382–388. [PubMed: 19067657]
12. Lunsford KE, Jayanshankar K, Eiring AM, Horne PH, Koester MA, Gao D, Bumgardner GL. Alloreactive (CD4-Independent) CD8+ T cells jeopardize long-term survival of intrahepatic islet allografts. Am J Transplant. 2008; 8(6):1113–1128. [PubMed: 18522544]
13. Rickels MR, Kamoun M, Kearns J, Markmann JF, Naji A. Evidence for allograft rejection in an islet transplant recipient and effect on beta-cell secretory capacity. J Clin Endocrinol Metab. 2007; 92(7):2410–2414. [PubMed: 17488791]
14. Giraldo JA, Weaver JD, Stabler CL. Enhancing Clinical Islet Transplantation through Tissue Engineeering Strategies. J Diabetes Sci Technol. 2010; 4(5):1238–1247. [PubMed: 20920446]
15. De Vos P, De Haan B, Pater J, Van Schilfgaarde R. Association between capsule diameter, adequacy of encapsulation, and survival of microencapsulated rat islet allografts. Transplantation. 1996; 62(7):893–899. [PubMed: 8878380]

16. Dionne KE, Colton CK, Yarmush ML. Effect of hypoxia on insulin secretion by isolated rat and canine islets of Langerhans. Diabetes. 1993; 42(1):12–21. [PubMed: 8420809]
17. Leung A, Ramaswamy Y, Munro P, Lawrie G, Nielsen L, Trau M. Emulsion strategies in the microencapsulation of cells: pathways to thin coherent membranes. Biotechnol Bioeng. 2005; 92(1):45–53. [PubMed: 15986491]
18. Headen DM, Aubry G, Lu H, Garcia AJ. Microfluidic-based generation of size-controlled, biofunctionalized synthetic polymer microgels for cell encapsulation. Adv Mater. 2014; 26(19): 3003–3008. [PubMed: 24615922]
19. Tomei AA, Manzoli V, Fraker CA, Giraldo J, Velluto D, Najjar M, Pileggi A, Molano RD, Ricordi C, Stabler CL, Hubbell JA. Device design and materials optimization of conformal coating for islets of Langerhans. Proc Natl Acad Sci U S A. 2014; 111(29):10514–10519. [PubMed: 24982192]
20. Gattas-Asfura KM, Stabler CL. Bioorthogonal layer-by-layer encapsulation of pancreatic islets via hyperbranched polymers. ACS Appl Mater Interfaces. 2013; 5(20):9964–9974. [PubMed: 24063764]
21. Rengifo HR, Giraldo JA, Labrada I, Stabler CL. Long-term survival of allograft murine islets coated via covalently stabilized polymers. Adv Healthc Mater. 2014; 3(7):1061–1070. [PubMed: 24497465]
22. Abuchowski A, McCoy JR, Palczuk NC, van Es T, Davis FF. Effect of covalent attachment of polyethylene glycol on immunogenicity and circulating life of bovine liver catalase. J Biol Chem. 1977; 252(11):3582–3586. [PubMed: 16907]
23. Abuchowski A, van Es T, Palczuk NC, Davis FF. Alteration of immunological properties of bovine serum albumin by covalent attachment of polyethylene glycol. J Biol Chem. 1977; 252(11):3578–3581. [PubMed: 405385]
24. Scott MD, Murad KL, Koumpouras F, Talbot M, Eaton JW. Chemical camouflage of antigenic determinants: stealth erythrocytes. Proc Natl Acad Sci U S A. 1997; 94(14):7566–7571. [PubMed: 9207132]
25. Panza JL, Wagner WR, Rilo HL, Rao RH, Beckman EJ, Russell AJ. Treatment of rat pancreatic islets with reactive PEG. Biomaterials. 2000; 21(11):1155–1164. [PubMed: 10817268]
26. Lee DY, Yang K, Lee S, Chae SY, Kim KW, Lee MK, Han DJ, Byun Y. Optimization of monomethoxy-polyethylene glycol grafting on the pancreatic islet capsules. J Biomed Mater Res. 2002; 62(3):372–377. [PubMed: 12209922]
27. Le Y, Scott MD. Immunocamouflage: The biophysical basis of immunoprotection by grafted methoxypoly(ethylene glycol) (mPEG). Acta Biomater. 2010; 6(7):2631–2641. [PubMed: 20109585]
28. Lee DY, Park SJ, Lee S, Nam JH, Byun Y. Highly poly(ethylene) glycolylated islets improve long-term islet allograft survival without immunosuppressive medication. Tissue Eng. 2007; 13(8): 2133–2141. [PubMed: 17516853]
29. Dong H, Fahmy TM, Metcalfe SM, Morton SL, Dong X, Inverardi L, Adams DB, Gao W, Wang H. Immuno-Isolation of Pancreatic Islet Allografts Using Pegylated Nanotherapy Leads to Long-Term Normoglycemia in Full MHC Mismatch Recipient Mice. PLoS One. 2012; 7(12):e50265. [PubMed: 23227162]
30. Lee DY, Lee S, Nam JH, Byun Y. Minimization of immunosuppressive therapy after islet transplantation: combined action of heme oxygenase-1 and PEGylation to islet. Am J Transplant. 2006; 6(8):1820–1828. [PubMed: 16780547]
31. Lee DY, Park SJ, Nam JH, Byun Y. A combination therapy of PEGylation and immunosuppressive agent for successful islet transplantation. J Control Release. 2006; 110(2):290–295. [PubMed: 16324765]
32. Nicolls MR, Gill RG. LFA-1 (CD11a) as a therapeutic target. Am J Transplant. 2006; 6(1):27–36. [PubMed: 16433753]
33. Nicolls MR, Coulombe M, Yang H, Bolwerk A, Gill RG. Anti-LFA-1 therapy induces long-term islet allograft acceptance in the absence of IFN-gamma or IL-4. J Immunol. 2000; 164(7):3627–3634. [PubMed: 10725719]

34. Berney T, Pileggi A, Molano RD, Poggioli R, Zahr E, Ricordi C, Inverardi L. The effect of simultaneous CD154 and LFA-1 blockade on the survival of allogeneic islet grafts in nonobese diabetic mice. Transplantation. 2003; 76(12):1669–1674. [PubMed: 14688513]
35. Arai K, Sunamura M, Wada Y, Takahashi M, Kobari M, Kato K, Yagita H, Okumura K, Matsuno S. Preventing effect of anti-ICAM-1 and anti-LFA-1 monoclonal antibodies on murine islet allograft rejection. Int J Pancreatol. 1999; 26(1):23–31. [PubMed: 10566155]
36. Fotino C, Pileggi A. Blockade of leukocyte function antigen-1 (LFA-1) in clinical islet transplantation. Curr Diab Rep. 2011; 11(5):337–344. [PubMed: 21755435]
37. Nicolls MR, Coulombe M, Beilke J, Gelhaus HC, Gill RG. CD4-dependent generation of dominant transplantation tolerance induced by simultaneous perturbation of CD154 and LFA-1 pathways. J Immunol. 2002; 169(9):4831–4839. [PubMed: 12391193]
38. Pileggi A, Molano RD, Berney T, Cattan P, Vizzardelli C, Oliver R, Fraker C, Ricordi C, Pastori RL, Bach FH, Inverardi L. Heme oxygenase-1 induction in islet cells results in protection from apoptosis and improved in vivo function after transplantation. Diabetes. 2001; 50(9):1983–1991. [PubMed: 11522663]
39. Pedraza E, Coronel MM, Fraker CA, Ricordi C, Stabler CL. Preventing hypoxia-induced cell death in beta cells and islets via hydrolytically activated, oxygen-generating biomaterials. Proc Natl Acad Sci U S A. 2012; 109(11):4245–4250. [PubMed: 22371586]
40. Buchwald P, Cechin SR, Weaver JD, Stabler CL. Experimental evaluation and computational modeling of the effects of encapsulation on the time-profile of glucose-stimulated insulin release of pancreatic islets. Biomed Eng Online. 2015; 14(1):1–14. [PubMed: 25564100]
41. Bottino R, Balamurugan AN, Bertera S, Pietropaolo M, Trucco M, Piganelli JD. Preservation of Human Islet Cell Functional Mass by Anti-Oxidative Action of a Novel SOD Mimic Compound. Diabetes. 2002; 51(8):2561–2567. [PubMed: 12145171]
42. Molano RD, Pileggi A, Berney T, Poggioli R, Zahr E, Oliver R, Ricordi C, Rothstein DM, Basadonna GP, Inverardi L. Prolonged Islet Allograft Survival in Diabetic NOD Mice by Targeting CD45RB and CD154. Diabetes. 2003; 52(4):957–964. [PubMed: 12663467]
43. Badell IR, Russell MC, Thompson PW, Turner AP, Weaver TA, Robertson JM, Avila JG, Cano JA, Johnson BE, Song M, Leopardi FV, Swygert S, Strobert EA, Ford ML, Kirk AD, Larsen CP. LFA-1-specific therapy prolongs allograft survival in rhesus macaques. J Clin Invest. 2010; 120(12):4520–4531. [PubMed: 21099108]
44. Wolf MT, Dearth CL, Ranallo CA, LoPresti ST, Carey LE, Daly KA, Brown BN, Badylak SF. Macrophage polarization in response to ECM coated polypropylene mesh. Biomaterials. 2014; 35(25):6838–6849. [PubMed: 24856104]
45. Schmittgen TD, Livak KJ. Analyzing real-time PCR data by the comparative C(T) method. Nat Protoc. 2008; 3(6):1101–1108. [PubMed: 18546601]
46. Wang RN, Paraskevas S, Rosenberg L. Characterization of Integrin Expression in Islets Isolated from Hamster, Canine, Porcine, and Human Pancreas. J Histochem Cytochem. 1999; 47(4):499–506. [PubMed: 10082751]
47. Murad KL, Mahany KL, Brugnara C, Kuypers FA, Eaton JW, Scott MD. Structural and functional consequences of antigenic modulation of red blood cells with methoxypoly(ethylene glycol). Blood. 1999; 93(6):2121–2127. [PubMed: 10068687]
48. Thomas F, Wu J, Contreras JL, Smyth C, Bilbao G, He J, Thomas J. A tripartite anoikis-like mechanism causes early isolated islet apoptosis. Surgery. 2001; 130(2):333–338. [PubMed: 11490368]
49. Zhang F, Kang ET, Neoh KG, Wang P, Tan KL. Reactive coupling of poly(ethylene glycol) on electroactive polyaniline films for reduction in protein adsorption and platelet adhesion. Biomaterials. 2002; 23(3):787–795. [PubMed: 11771698]
50. Hansson KM, Tosatti S, Isaksson J, Wetterö J, Textor M, Lindahl TL, Tengvall P. Whole blood coagulation on protein adsorption-resistant PEG and peptide functionalised PEG-coated titanium surfaces. Biomaterials. 2005; 26(8):861–872. [PubMed: 15353197]
51. Nicolls MR, Coulombe M, Yang H, Bolwerk A, Gill RG. Anti-LFA-1 Therapy Induces Long-Term Islet Allograft Acceptance in the Absence of IFN-γ or IL-4. J Immunol. 2000; 164(7):3627–3634. [PubMed: 10725719]

52. Nanji SA, Hancock WW, Anderson CC, Adams AB, Luo B, Schur CD, Pawlick RL, Wang L, Coyle AJ, Larsen CP, Shapiro AMJ. Multiple Combination Therapies Involving Blockade of ICOS/B7RP-1 Costimulation Facilitate Long-Term Islet Allograft Survival. Am J Transplant. 2004; 4(4):526–536. [PubMed: 15023144]
53. Gao W, Demirci G, Strom TB, Li XC. Stimulating PD-1-negative signals concurrent with blocking CD154 co-stimulation induces long-term islet allograft survival. Transplantation. 2003; 76(6):994–999. [PubMed: 14508368]
54. Tedesco D, Haragsim L. Cyclosporine: a review. J Transplant. 2012; 2012:230386. [PubMed: 22263104]
55. Kitchens WH, Haridas D, Wagener ME, Song M, Ford ML. Combined costimulatory and leukocyte functional antigen-1 blockade prevents transplant rejection mediated by heterologous immune memory alloresponses. Transplantation. 2012; 93(10):997–1005. [PubMed: 22475765]
56. Ford ML, Larsen CP. Translating costimulation blockade to the clinic: lessons learned from three pathways. Immunol Rev. 2009; 229(1):294–306. [PubMed: 19426229]
57. Lacy PE, Davie JM, Finke EH. Effect of Culture on Islet Rejection. Diabetes. 1980; 29(Supplement 1):93–97. [PubMed: 6766417]
58. Opelz G, Terasaki PI. Lymphocyte Antigenicity Loss with Retention of Responsiveness. Science. 1974; 184(4135):464–466. [PubMed: 4274306]
59. Pileggi A, Molano RD, Berney T, Ichii H, San Jose S, Zahr E, Poggioli R, Linetsky E, Ricordi C, Inverardi L. Prolonged allogeneic islet graft survival by protoporphyrins. Cell Transplant. 2005; 14(2–3):85–96. [PubMed: 15881418]
60. Citro A, Cantarelli E, Piemonti L. Anti-Inflammatory Strategies to Enhance Islet Engraftment and Survival. Curr Diab Rep. 2013; 13(5):733–744. [PubMed: 23912763]
61. Imai Y, Dobrian AD, Morris MA, Nadler JL. Islet inflammation: a unifying target for diabetes treatment? Trends Endocrinol Metab. 2013; 24(7):351–360. [PubMed: 23484621]
62. Sahraoui A, Jensen KK, Ueland T, Korsgren O, Foss A, Scholz H. Anakinra and tocilizumab enhance survival and function of human islets during culture: implications for clinical islet transplantation. Cell Transplant. 2013; 23(10):1199–1211. [PubMed: 23635711]
63. Xiao X, Gittes GK. Concise Review: New Insights Into the Role of Macrophages in beta- Cell Proliferation. Stem Cells Transl Med. 2015; 4(6):655–658. [PubMed: 25900729]
64. Kaufman DB, Gores PF, Field MJ, Farney AC, Gruber SA, Stephanian E, Sutherland DE. Effect of 15-deoxyspergualin on immediate function and long-term survival of transplanted islets in murine recipients of a marginal islet mass. Diabetes. 1994; 43(6):778–783. [PubMed: 8194663]
65. Bottino R, Fernandez LA, Ricordi C, Lehmann R, Tsan MF, Oliver R, Inverardi L. Transplantation of allogeneic islets of Langerhans in the rat liver: effects of macrophage depletion on graft survival and microenvironment activation. Diabetes. 1998; 47(3):316–323. [PubMed: 9519734]
66. Ford ML, Adams AB, Pearson TC. Targeting co-stimulatory pathways: transplantation and autoimmunity. Nat Rev Nephrol. 2014; 10(1):14–24. [PubMed: 24100403]
67. Vergani A, Fotino C, D'Addio F, Tezza S, Podetta M, Gatti F, Chin M, Bassi R, Molano RD, Corradi D, Gatti R, Ferrero ME, Secchi A, Grassi F, Ricordi C, Sayegh MH, Maffi P, Pileggi A, Fiorina P. Effect of the Purinergic Inhibitor Oxidized ATP in a Model of Islet Allograft Rejection. Diabetes. 2013; 62(5):1665–1675. [PubMed: 23315496]
68. Martin BM, Samy KP, Lowe MC, Thompson PW, Cano J, Farris AB, Song M, Dove CR, Leopardi FV, Strobert EA, Jenkins JB, Collins BH, Larsen CP, Kirk AD. Dual Islet Transplantation Modeling of the Instant Blood-Mediated Inflammatory Reaction. Am J Transplant. 2015; 15(5): 1241–1252. [PubMed: 25702898]
69. Oberbarnscheidt MH, Zeng Q, Li Q, Dai H, Williams AL, Shlomchik WD, Rothstein DM, Lakkis FG. Non-self recognition by monocytes initiates allograft rejection. J Clin Invest. 124(8):3579–3589.
70. Dong H, Zhang Y, Song L, Kim DS, Wu H, Yang L, Li S, Morgan KA, Adams DB, Wang H. Cell-permeable Peptide Blocks TLR4 signaling and Improves Islet Allograft Survival. Cell Transplant. 2016; 25(7):1319–1329. [PubMed: 26771084]
71. Martinez FO, Gordon S. The M1 and M2 paradigm of macrophage activation: time for reassessment. F1000Prime Rep. 2014; 6

72. Mantovani A, Sozzani S, Locati M, Allavena P, Sica A. Macrophage polarization: tumor-associated macrophages as a paradigm for polarized M2 mononuclear phagocytes. Trends Immunol. 2002; 23(11):549–555. [PubMed: 12401408]

73. Savage NDL, de Boer T, Walburg KV, Joosten SA, van Meijgaarden K, Geluk A, Ottenhoff THM. Human Anti-Inflammatory Macrophages Induce Foxp3+GITR+CD25+ Regulatory T Cells, Which Suppress via Membrane-Bound TGFβ-1. J Immunol. 2008; 181(3):2220–2226. [PubMed: 18641362]

74. Chauhan SK, Saban DR, Lee HK, Dana R. Levels of Foxp3 in Regulatory T Cells Reflect Their Functional Status in Transplantation. J Immunol. 2009; 182(1):148–153. [PubMed: 19109145]

75. Taylor PA, Noelle RJ, Blazar BR. Cd4+Cd25+ Immune Regulatory Cells Are Required for Induction of Tolerance to Alloantigen via Costimulatory Blockade. J Exp Med. 2001; 193(11): 1311–1318. [PubMed: 11390438]

76. Ricordi C, Goldstein JS, Balamurugan AN, Szot GL, Kin T, Liu C, Czarniecki CW, Barbaro B, Bridges ND, Cano J, Clarke WR, Eggerman TL, Hunsicker LG, Kaufman DB, Khan A, Lafontant D-E, Linetsky E, Luo X, Markmann JF, Naji A, Korsgren O, Oberholzer J, Turgeon NA, Brandhorst D, Friberg AS, Lei J, Wang L-j, Wilhelm JJ, Willits J, Zhang X, Hering BJ, Posselt AM, Stock PG, Shapiro AMJ. National Institutes of Health–Sponsored Clinical Islet Transplantation Consortium Phase 3 Trial: Manufacture of a Complex Cellular Product at Eight Processing Facilities. Diabetes. 2016; 65(11):3418–3428. [PubMed: 27465220]

77. Miura S, Teramura Y, Iwata H. Encapsulation of islets with ultra-thin polyion complex membrane through poly(ethylene glycol)-phospholipids anchored to cell membrane. Biomaterials. 2006; 27(34):5828–5835. [PubMed: 16919725]

78. Kozlovskaya V, Zavgorodnya O, Chen Y, Ellis K, Tse HM, Cui X, Thompson JA, Kharlampieva E. Ultrathin Polymeric Coatings Based on Hydrogen-Bonded Polyphenol for Protection of Pancreatic Islet Cells. Adv Funct Mater. 2012; 22(16):3389–3398. [PubMed: 23538331]

79. Wilson JT, Krishnamurthy VR, Cui W, Qu Z, Chaikof EL. Noncovalent cell surface engineering with cationic graft copolymers. J Am Chem Soc. 2009; 131(51):18228–18229. [PubMed: 19961173]

Statement of Significance

We believe this study is important and of interest to the biomaterials and transplant community for several reasons: 1) it provides an optimized protocol for the PEGylation of islets, with minimal impact on the coated islets, which can be easily translated for clinical applications; 2) this optimized protocol demonstrates the benefits of islet PEGylation in providing modest immunosuppression in a murine model; 3) this work demonstrates the combinatory impact of PEGylation with short-course immunotherapy (via LFA-1 blockage), illustrating the capacity of PEGylation to complement existing immunotherapy; and 4) it suggests macrophage phenotype shifting as the potential mechanism for this observed benefit.

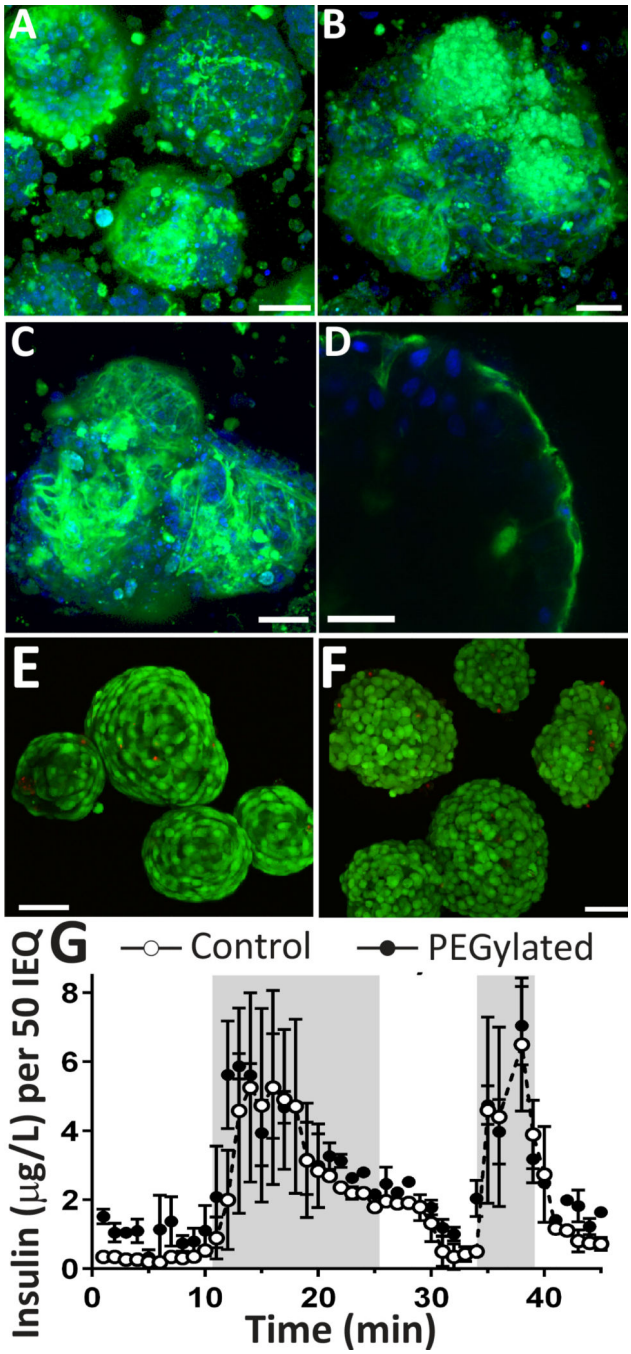

Figure 1. Assessment of coating, viability, and function of PEGylated pancreatic rodent islets

Representative multi-slice projection confocal images of representative islets from three separate islet isolations (A, B, and C), demonstrating grafting of NHS-PEG-FITC onto pancreatic islets, with variation in intensity of coating. D) Single slice confocal image of PEGylated islet, illustrating conjugation of PEG to the islet periphery (NHS-PEG-FITC, green and Hoechst nuclei counterstain, blue). Representative multi-slice projection confocal microscopy images of control (E) and PEGylated islets (F) stained with live/dead (green = viable; red = dead). G) Dynamic glucose stimulated insulin secretion (GSIR) (low glucose

(10 min) → high glucose (15 mins) → low glucose (10 mins) → KCL (5 min) → low glucose (10 mins) of PEGylated islets (filled circles), compared to control (open circles); n = 3. Scale = 50 μm Error bars = STD

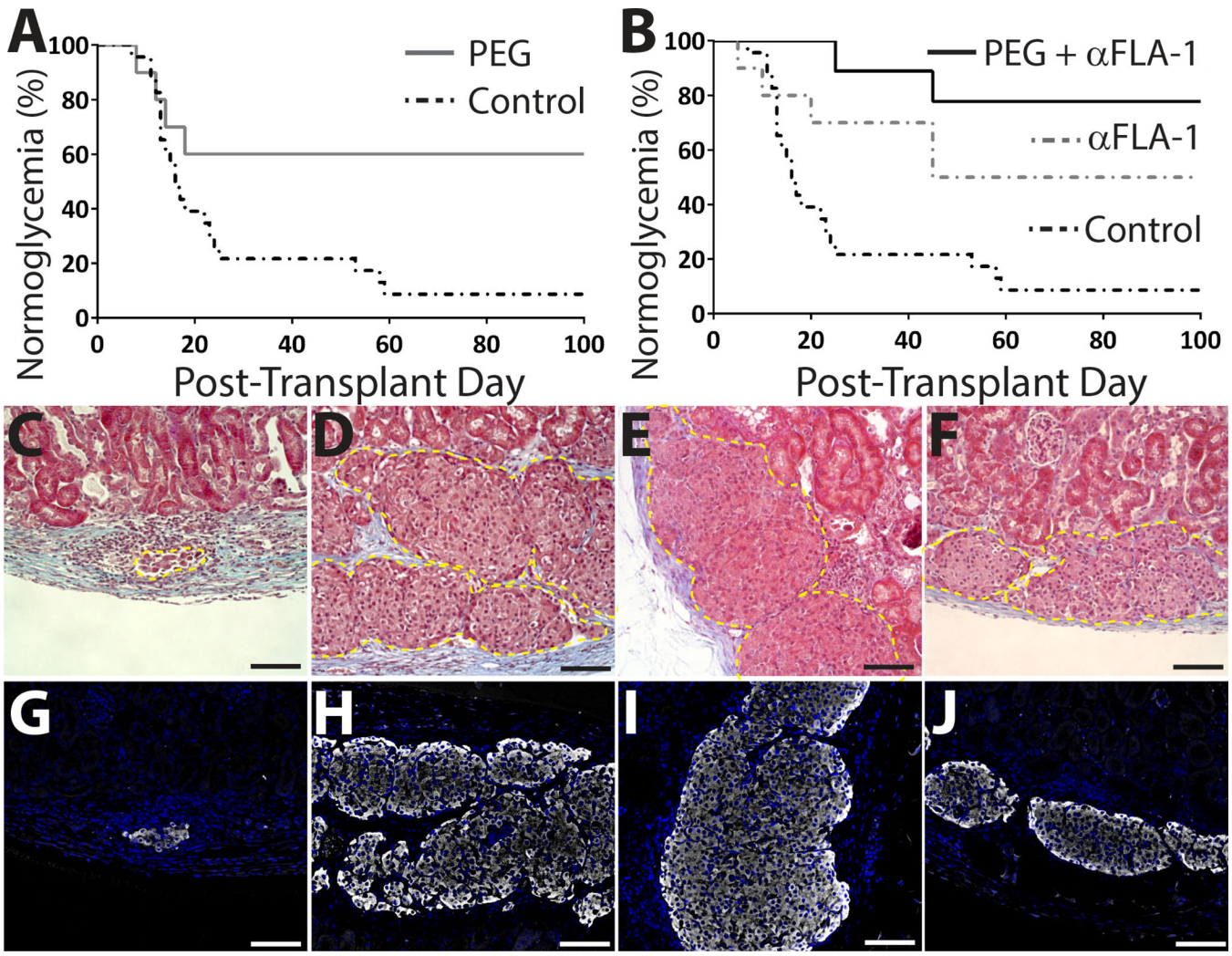

Figure 2. Enhanced engraftment of PEGylated islets and complementary impact of short-course anti-LFA-1 on PEGylated islet survival

A) A significant percentage of PEGylated islet grafts (n = 11) exhibited long-term function, as demonstrated by % normoglycemia, compared to controls (n = 24) ($P = 0.01$). B) Combination of PEGylation with LFA-1 blockade (n = 13) resulted in a higher percentage of grafts functioning long term ($P = 0.003$) when compared to controls, while LFA-1 blockade only (n = 10) resulted in survival rates equivalent to PEGylated islets alone ($P = 0.80$). Representative images of control islets (C,G), explanted 20 d post-transplant after destabilization of graft, and PEGylated islets (D,H), unmodified islets with anti-LFA-1 (E,I) or PEGylated islets with anti-LFA-1 (F,J) all electively explanted 193 d post-transplant. Explants were stained via trichrome (C-F; yellow dashed line outline transplanted islets) and immunofluorescence (G-J; insulin: white; nuclei DAPI: blue). Scale bar = 100 μm.

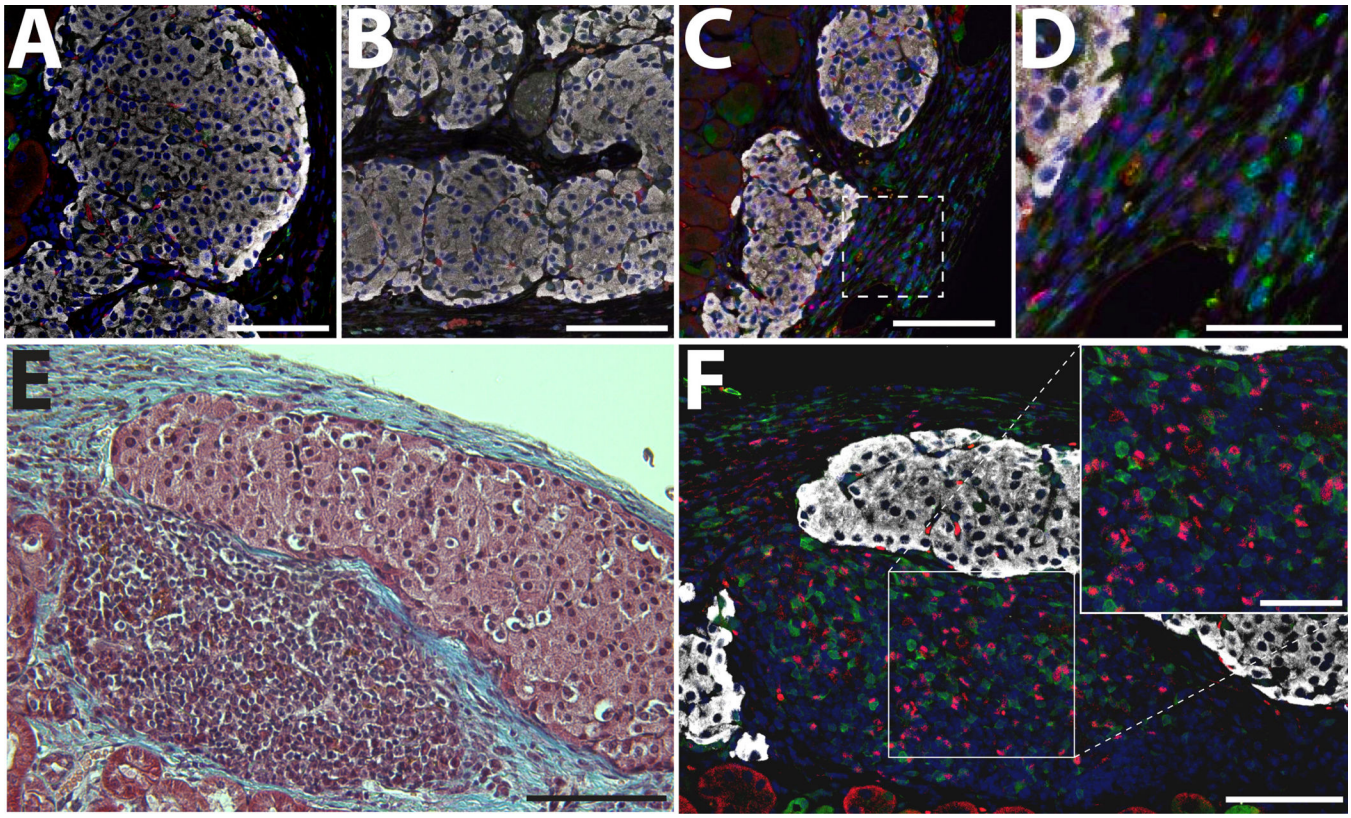

Figure 3. Immunofluorescence staining of grafts functioning long term

Representative images of successful grafts functioning long-term for anti-LFA-1 only (A), PEGylated only (B), and anti-LFA-1 and PEGylated islets (C). D) Higher magnification of graft in C (box highlights area). E-F) Representative tri-chrome and immunofluorescence stained explant demonstrating mononuclear accumulation. Grafts were immunostained for CD3 (green), FoxP3 (red), and Insulin (white); counterstained with DAPI (blue). A–C, E: scale bar = 100 μm. D & F: scale bar = 50 μm.

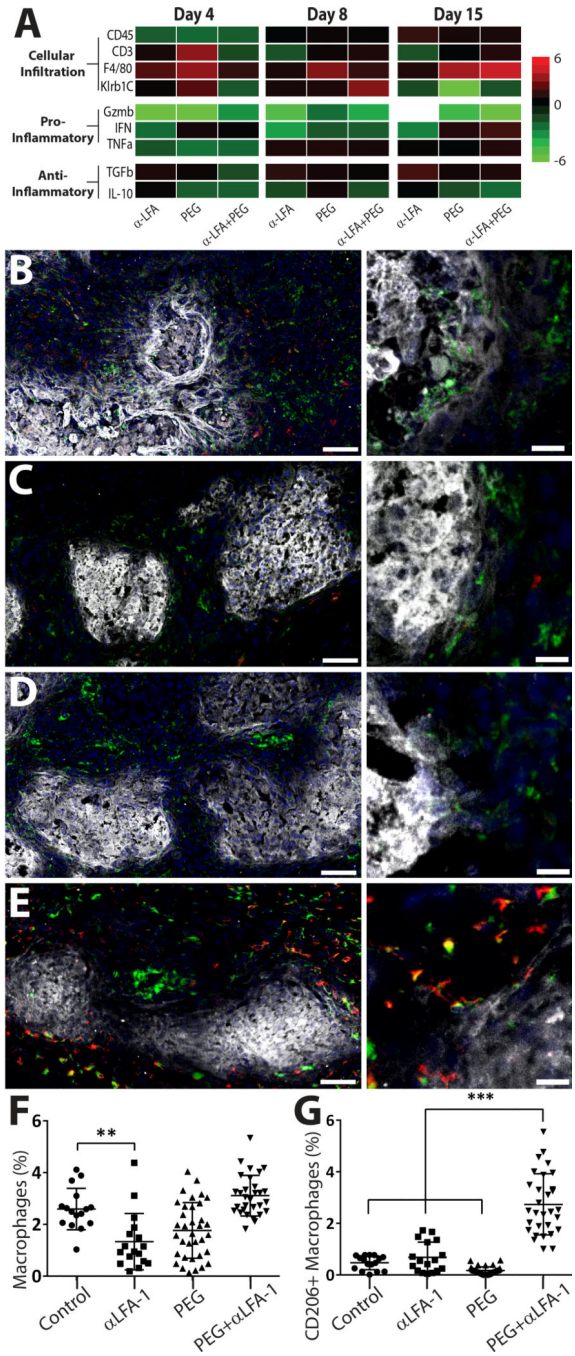

Figure 4. Evaluation of early host responses to implants reveal modulation of inflammatory events

qPCR analysis summarizing the impact of PEGylation, anti-LFA-1, and anti-LFA-1 + PEGylation on the implant microenvironment (A). Gene are expressed as fold control (n = 4 per group). Immunohistochemistry of grafts electively terminated 8 days post-transplantation and immunostained for general macrophage marker CD68 (green), macrophage M2 marker CD206 (red), and insulin (white); counterstained with DAPI nuclei stain (blue). Representative images of grafts from control (B), PEGylated only (C), anti-LFA-1 only (D), and the combination of anti-LFA-1 and PEGylated islets (E) groups at low

(left) and high (right) magnification. Scale bar = 50 μm (left) or 20 μm (right). IHC quantification of macrophages (CD68+, F) and M2 phenotype macrophages (CD206+CD68+, G); n > 15 ** P < 0.01; *** P<0.001

Table 1

Listing of primers used for qPCR analysis of grafts explanted via laser capture microdissection.

Target	Assay ID
Ptprc (CD45)	Mm01293577_m1
Cd3d	Mm00442746_m1
Emr1(F4/80)	Mm00802529_m1
Klrb1c (Nk1.1)	Mm00824341_m1
GzmB	Mm00442834_m1
IFNγ	Mm01168134_m1
TNFα	Mm00443260_g1
TGFβ-1	Mm01178820_m1
IL-10	Mm00439614_m1